Suppression of the metal-insulator transition in the spinel $Cu_{1-x}In_xIr_2S_4$ system

Guanghan Cao,* Xiaofeng Xu, and Zhengkuan Jiao
Department of Physics, Zhejiang University, Hangzhou 310027, People's Republic of China

Hideaki Kitazawa and Takehiko Matsumoto
National Institute for Materials Science, Sengen 1-2-1, Tsukuba, Ibaraki 305-0047, Japan

Chunmu Feng
Test and Analysis Center, Zhejiang University, Hangzhou 310027, People's Republic of China
(Received 17 October 2004; revised manuscript received 2 May 2005; published 30 September 2005)

The thiospinel $Cu_{1-x}In_xIr_2S_4(0 \leqslant x \leqslant 0.25)$ system was studied by the measurements of crystal structure, electrical resistivity, and magnetic susceptibility. The parent compound was known to exhibit an intriguing first-order metal-insulator (MI) transition with a simultaneous spin-dimerization and charge ordering at ~230 K with decreasing temperature. Upon indium doping on the copper site, the conduction holes of the metallic phase are depleted, or the doped electrons occupy the antibonding state of the insulating phase, suppressing the MI transition. Moreover, the first-order transition is changed into a higher-order one for $x \geqslant 0.2$. Our experimental data suggest that the higher-order phase transition is associated with an electronic transformation from small polarons to small bipolarons. Comparing the doping effects of Zn, Cd, and In, we found that the variations of the electrical and magnetic properties depend on the lattice size, i.e., the suppression of the MI transition becomes weaker for an enlarged lattice. This lattice size effect is mainly explained in terms of the electron-phonon interactions, which is enhanced by the band narrowing due to the larger ionic size of the dopants.

DOI: 10.1103/PhysRevB.72.125128 PACS number(s): 71.30.+h, 71.38.−k, 72.80.Ga

I. INTRODUCTION

The spinel-type compound $CuIr_2S_4$ undergoes an intriguing first-order MI transition at $T_{MI} \sim 230$ K with decreasing temperature.[1,2] The high-temperature metallic phase crystallizes in a normal cubic spinel structure with the Cu, Ir cations occupying tetrahedral and octahedral sites of AB_2X_4, respectively. On the other hand, the crystal structure of the low-temperature insulating phase is distorted in such an unusual way that charge (Ir^{3+}/Ir^{4+}) ordering and spin ($S=1/2$ for Ir^{4+}) dimerization take place simultaneously.[3] The unique spin-dimerization in a three-dimensional structure as well as the complex charge-ordering pattern that consists of $Ir_8^{3+}S_{24}$ and $Ir_8^{4+}S_{24}$ octamers makes the spinel very interesting and challenging. Moreover, $CuIr_2S_4$ shows additional anomalous characteristics in the pressure effect on T_{MI},[4] the transport properties,[5,6] electronic structures,[7–9] x-ray-induced phase transition[10,11] and doping-induced superconductivity.[12–14] Therefore, $CuIr_2S_4$ represents another model system on the topic of MI transitions[15,16] in the field of condensed matter physics.

$CuIr_2S_4$ belongs to 5*d*-transition-metal sulfides. The average *d*-*d* Coulomb energy of Ir 5*d* electrons is about 3.5 eV, obviously smaller than those of 3*d* transition-metal oxides.[17] On the other hand, the hybridization between Ir 5*d* and S 3*p* orbitals is very strong, resulting in a large $d\gamma$-$d\varepsilon$ splitting and a broad $d\varepsilon$ band of 7.0 eV.[18] Therefore, the electron correlation would not play the dominant role in the MI transition. It was shown that the Fermi level E_F lies near the top of the $d\varepsilon$ band, leading to the metallic state with the hole conduction for the cubic spinel $CuIr_2S_4$.[18] Note that the copper is monovalent, as revealed by the photoemission study,[7] the energy-band calculations,[18] and the Cu NMR measurement.[19] The electronic configuration of Ir in $CuIr_2S_4$ is $5d\varepsilon^{5.5}$, or more precisely, $[e_g^4][a_{1g}^{1.5}]$ when considered the distortion of the IrS_6 octahedra. So, the highest-occupying a_{1g} state should be regarded as quarter-occupying with holes, which seems to be important for the simultaneous charge ordering and spin-dimerization.[20] Very recently, band-structure calculations[21] for the insulating phase of $CuIr_2S_4$ reveals that the band gap opening is due to the bonding-antibonding splitting of the atomic $d\varepsilon$ orbitals at the dimerized Ir sites. However, the driving force of the MI transition remains unclear.

An elemental substitution study may give useful information on the physical mechanism as well as a route to new materials. In the present thiospinel system, elemental substitutions on different crystallographic sites with specific elements have been performed.[13,22–26] Among them, the *A*-site substitution hardly changes the IrS_6-octahedron framework that determines the electronic structure of the valence bands, therefore, this kind of substitution brings the effects of the lattice size and the carrier filling. For example, Zn^{2+} substitution for Cu^+ depletes the hole carriers of the metallic $CuIr_2S_4$ phase, resulting in the suppression of the MI transition and the appearance of superconductivity.[13] Substitution for Cu^+ by a larger cation Cd^{2+} similarly decreases the hole concentration in the metallic phase, however, a bipolaronic state appears instead of the superconducting one.[26] So, the electronic property is determined not only by the hole depletion but also by the lattice size. In order to further understand this finding, one needs to make the Cu-site substitution by the nonmagnetic cation with different size and valence. In^{3+} has the same electronic configuration nd^{10}, whose energy

level is far below E_F, as those of Cu^+, Zn^{2+}, and Cd^{2+}, but it is trivalent and it has intermediate size. Therefore, we carried out the study on the $Cu_{1-x}In_xIr_2S_4$ system. The result forms a systematic understanding on the suppression and evolution of the MI transition by the hole depletion and the lattice size, which suggests that the strong electron-lattice interaction plays an important role for the MI transition in the thiospinel system.

II. EXPERIMENTS

Polycrystalline samples of $Cu_{1-x}In_xIr_2S_4$($x=0,0.025,0.05,0.1,0.15,0.2,0.25,0.3,0.5$) were prepared by a solid-state reaction method. First, mixture of Cu (99.99%), Ir (99.99%), In (99.99%), and S (99.999%) powders with the nominal stoichiometry was sealed in an evacuated quartz ampoule. Then, the sealed ampoule was heated slowly to 1023 K, holding for 24 hours, followed by the calcination at 1373 K for a period of 4 days. In order to increase the indium solubility, samples were quenched.[26] The resulting powder was subsequently ground and pressed into pellets with the pressure of $\sim 2000\ kg/cm^2$. Finally, the pellets were sintered in an evacuated quartz ampoule again at 1373 K for 48 hours and then quenched.

Powder x-ray diffraction (XRD) was carried out at room temperature with Cu $K\alpha$ radiation by employing a RIGAKU x-ray diffractometer. The crystal structure parameters were refined by the RIETAN Rietveld analysis program.[27] The electrical resistivity (ρ) was measured by the standard four-probe method. The magnetization of samples was measured by using a Quantum Design SQUID magnetometer. The measurement was carried out using about 100 mg samples in both cooling and heating processes between 1.8 K and 300 K under the applied field of 1000 Oe. The background arising from the sample holder was measured in advance and then subtracted.

III. RESULTS AND DISCUSSION

A. Structural properties

Powder XRD measurements indicated that samples of $Cu_{1-x}In_xIr_2S_4$ with $0 \leqslant x \leqslant 0.25$ contained only spinel single phase. When $x \geqslant 0.3$, however, impurities started to appear. So, our study was limited to the range of $0 \leqslant x \leqslant 0.25$. Figure 1 shows the XRD pattern of the $x=0.25$ sample, in which the structure refinement has been made using the Rietveld analysis program.[27] The refinement demonstrates that the $Cu_{1-x}In_xIr_2S_4$ system crystallizes in normal spinel structure with the space group of $Fd\bar{3}m$, in which Cu and Ir occupy A and B sites, respectively. The occupancy of indium was investigated by assuming that In^{3+} and Ir^{3+} could occupy both A and B sites. The refinement for $x=0.25$ sample showed that In^{3+} occupancy at the A site was 0.22(2). For other samples it was shown that more than 90% of In^{3+} occupies the A site. The weighted-pattern factor R_{wp} for all the monophasic samples is in the range of 7.3% to 10.0%, and the parameter S that reflects "the goodness of the fitting" is around 1.8, indicating the reliability of structural refinements.

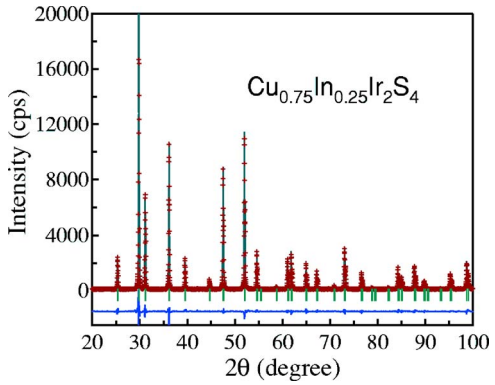

FIG. 1. (Color online) Profile of the room-temperature XRD Rietveld refinement for the sample of $Cu_{0.75}In_{0.25}Ir_2S_4$.

As we know, the crystal structure of the cubic spinel is characterized by the lattice constant a and the structural parameter u which determines the atomic position of sulfur at (u,u,u). Figure 2 shows the crystal structure parameters as a function of indium content. It can be seen that both a and u increase almost linearly with increasing indium content. The lattice expansion is due to the hole-filling (or, hole-depletion) effect[13] as well as the larger size of In^{3+} than that of Cu^+. The value of parameter u would be 0.375 in the ideal case of IrS_6 regular-octahedron coordination. In the present system, $u \approx 0.386$, indicating the stretch of IrS_6 octahedra along $\langle 111 \rangle$ directions. This leads to a negative trigonal coordination for Ir, which introduces a small splitting of the $t_{2g}(d\varepsilon)$ level into e_g and a_{1g} levels. Moreover, the increase of u also results in

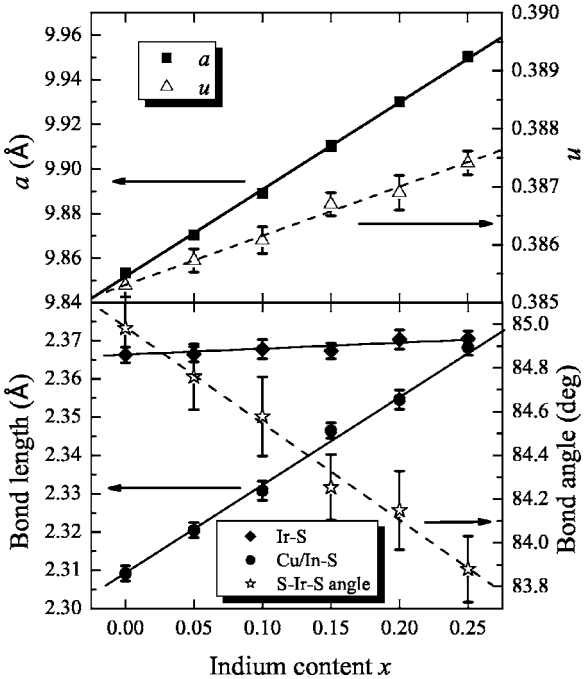

FIG. 2. Crystal structure parameters as a function of indium content in the $Cu_{1-x}In_xIr_2S_4$ system. The upper panel shows the lattice constant a and the parameter u, while the lower panel shows the interatomic distances and the S—Ir—S bond angle. The lines are guides to the eye.

the deviation of S—Ir—S bond angle from 90°, which weakens the $d\varepsilon$-p_π hybridization.

The bond distance and bond angle are thought to be the important structural parameters for the related interatomic hybridization. From the lattice geometry, the Cu/In—S interatomic distance d_{AX} can be expressed as

$$d_{AX} = \sqrt{3}a(u - 0.25). \quad (1)$$

On the other hand, the Ir—S bond length d_{BX} can be calculated using

$$d_{BX} = a\sqrt{0.0625 - 0.5(u - 0.375) + 3(u - 0.375)^2}. \quad (2)$$

One of the S—Ir—S bond angles (the small one) Θ can also be obtained by

$$\sin(\Theta/2) = 0.5d_{XX1}/d_{BX}, \quad (3)$$

where the short S—S bond distance is obtained by

$$d_{XX1} = 2\sqrt{2}a(0.5 - u). \quad (4)$$

As can be seen in the lower panel of Fig. 2, the Cu/In—S interatomic distance increases obviously, while the Ir—S bond length does not increase so much with the indium doping. This is in fact due to the distortion of the IrS_6 octahedra, which can be seen from the variations of the S—Ir—S band angle. It is here stressed that the related energy band such as the $d\varepsilon$-p_π bands should be narrowed due to the weakening of the hybridizations.

B. Electrical resistivity

The temperature dependence of resistivity in $Cu_{1-x}In_xIr_2S_4 (0 \leqslant x \leqslant 0.25)$ is shown in Fig. 3. As can be seen, the parent compound $CuIr_2S_4$ undergoes an abrupt MI transition identified by a three-order jump in resistivity around 230 K with a thermal hysteresis. Upon the indium doping, the MI transition temperature T_{MI} shifts to lower temperatures, and the resistivity jump becomes smaller. In other words, the MI transition in the parent compound is suppressed by the indium doping. It is noted that the thermal hysteresis in the transition disappears for $x \geqslant 0.2$, suggesting that the first-order transition is changed into a higher-order one. The higher-order transition temperature is here labelled T^*, defined as the inflexion point in the $\log_{10}\rho$-T curve.

Let us investigate the change of the high-temperature metallic state in some more details. First, the room-temperature resistivity increases monotonically with the indium doping. This is mainly due to the hole depletion, since the conductivity is proportional with the carrier concentration n_h (stronger evidence will be given in the magnetic susceptibility measurement below). Note that each indium atom depletes two holes, therefore, n_h is $0.5(1-2x)$ per Ir atom, according to the ideal stoichiometry of $Cu_{1-x}In_xIr_2S_4$. Second, the temperature coefficient of the resistivity (TCR) at room temperature decreases with the indium doping, and it changes the sign at $x \sim 0.2$, as shown in the magnifying plot of Fig. 3. The semiconductinglike conduction at the high temperature range in $x \sim 0.2$ samples is rather striking, because the carrier concentration is still high enough (0.3 per Ir atom). As a

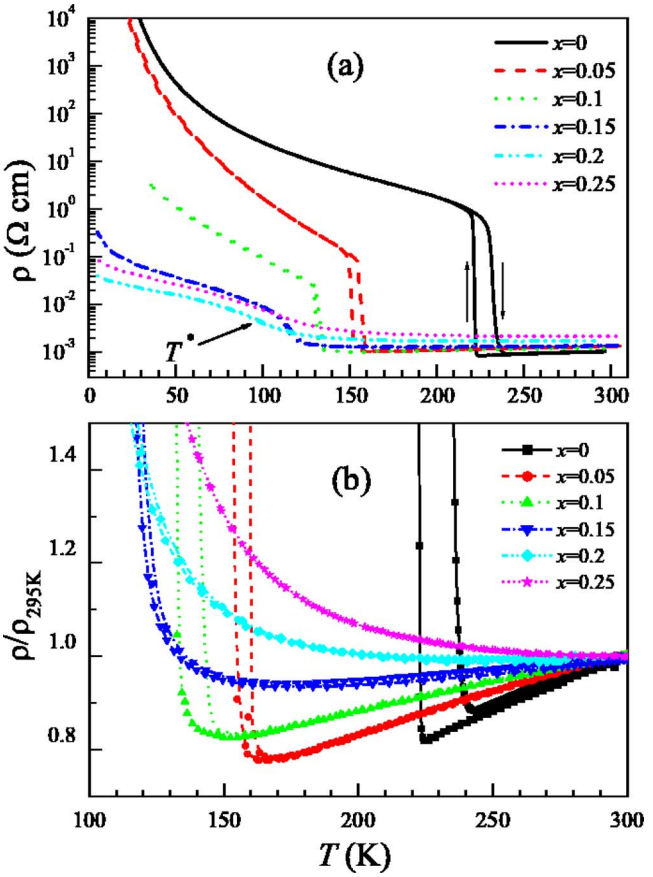

FIG. 3. (Color online) Temperature dependence of resistivity for the $Cu_{1-x}In_xIr_2S_4$ samples. Note that the upper panel uses the logarithmic scale for the resistivity axis. The lower panel shows the normalized resistivity in the high temperature range.

comparison in the $Cu_{1-x}Zn_xIr_2S_4$ system, metallic conduction is robust at room temperature up to $x \sim 0.9$ (i.e., $n_h \sim 0.05$ per Ir atom).[13] Finally, the sign change of the TCR coincides with the change of the transition order. Both occur at $x \sim 0.2$.

The metal-semiconductor transition induced by the hole depletion was also observed in the $Cu_{1-x}Cd_xIr_2S_4$ system, where the high-temperature semiconducting phase was tentatively called "polaronic semiconductor."[26] In fact, the polaronic semiconductor can be distinguished from the conventional semiconductor by the electrical transport behavior.[28] Resistivity of conventional semiconductor obeys the Arrhenius relation

$$\rho = A \exp\left(\frac{E_a}{k_B T}\right), \quad (5)$$

where E_a represents the activated energy and k_B is the Boltzman's constant. For adiabatic small-polaron hopping, however, the resistivity is given by[28]

$$\rho = \frac{k_B}{\nu e^2 d^2 n_{SP}} T \exp\left(\frac{E_0}{k_B T}\right), \quad (6)$$

where E_0 is the hopping energy, ν is the optical phonon or attempt frequency, e is the charge of the hole, d is the dis-

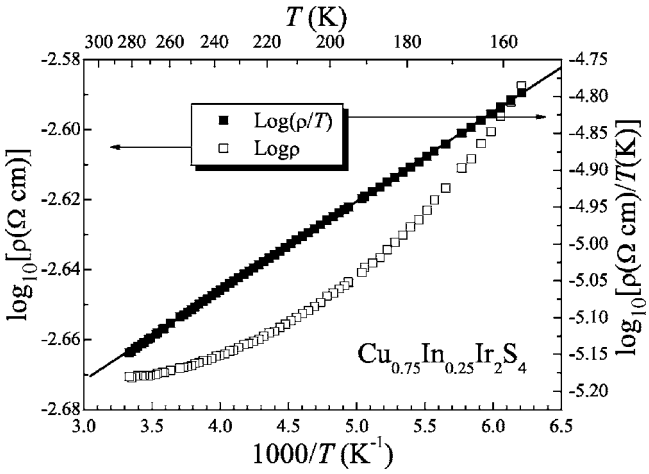

FIG. 4. High temperature resistivity in the $Cu_{0.75}In_{0.25}Ir_2S_4$, fitted in terms of the activated conduction [Eq. (5)] and the small polaron hopping conduction [Eq. (6)].

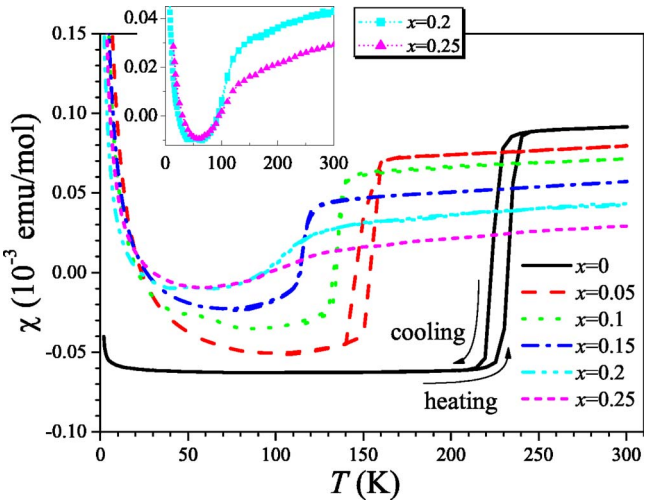

FIG. 5. (Color online) Temperature dependence of magnetic susceptibility for $Cu_{1-x}In_xIr_2S_4$ samples. The applied field is 1000 Oe.

tance between the hopping sites (the nearest Ir—Ir distance, being $\sqrt{2}a/4$), and n_{SP} is the density of small polarons. Figure 4 plots the high-temperature resistivity according to Eq. (5) and Eq. (6), respectively, for the $x=0.25$ sample. Obviously, the resistivity data agree the small-polaron hopping much better, suggesting the small polaron formation. The hopping energy is fitted to be 280 K and the attempt frequency is about 3.8×10^{11} Hz.

It is shown in Fig. 3 that the resistivity increases rapidly at T^* for the $x=0.25$ sample. We argue that this is due to the formation of small bipolarons (more evidence will be given in the next section). The formation of small bipolaron results in the decrease of the carrier (small polaron) concentration. On the other hand, since the conduction of small bipolarons is associated with the two carriers to hop to second neighbors, which is a higher-order process, one expects that the conductivity coming from the bipolaron pair breaking is small.[29] Therefore, one can see a rapid increase in resistivity at T^*.

C. Magnetic susceptibility

Figure 5 shows the temperature dependence of magnetic susceptibility (χ) in the $Cu_{1-x}In_xIr_2S_4(0\leqslant x\leqslant 0.25)$ system. The MI transition in the parent compound $CuIr_2S_4$ is characterized by the abrupt drop in magnetic susceptibility with a thermal hysteresis. This is due to the quenching of Pauli paramagnetic susceptibility in the metallic state, while in the insulating phase Ir^{4+} is dimerized in spin singlet. With the indium doping, it can be seen that T_{MI} first decreases rapidly, and then decreases steadily in accordance with the resistivity result. Similarly, the thermal hysteresis in the transition disappears for $x\geqslant 0.2$, suggesting the change of the transition order. The thermal hysteresis for the MI transition is associated with the structural phase transition from cubic to tetragonal,[2] or strictly speaking from cubic to triclinic,[3] in the parent compound. In the triclinic phase, ordered Ir^{4+} dimers form. We thus argue that such a structural phase transition should not occur for $x\geqslant 0.2$ because of the disappearance of thermal hysteresis. As a comparison, in a similar system of $Cu_{1-x}Zn_xIr_2S_4$,[13] the thermal hysteresis can be observed as long as the structural phase transition occurs. Nevertheless, we expect the detailed low-temperature XRD and NMR studies which will be able to check the point for the present system in the future.

One notes that the drop of χ can still be seen for $x\geqslant 0.2$. This suggests that disordered Ir^{4+} dimers (small bipolarons) forms below T^*. At lower temperatures, χ increases rapidly with decreasing temperature, obeying Curie-Weiss law. The effective magnetic moment is only about $0.1\mu_B$ per unit formula, which is probably attributed to the lattice imperfections.

One can also see from Fig. 5 that the high-temperature susceptibility decreases with increasing the indium content. Since the magnetic susceptibility in the metallic state is dominated by the Pauli paramagnetism with $\chi_{Pauli}=\mu_B^2N(E_F)$, and the Fermi level lies near the top of the valence band, the decrease in the magnetic susceptibility means that holes are filled by the extra electrons coming from the indium doping. Figure 6 shows the room-temperature susceptibility as a function of hole filling x' or hole concentration n_h by the different doping with Zn^{2+}, Cd^{2+}, and In^{3+}, respectively. Here, x' is defined as the decrease of hole concentration (per Ir atom) by the A-site doping, i.e., $x'=x$ for the In doping, while $x'=x/2$ for Zn and Cd doping. According to our previous study, $\chi_{Pauli}\approx\chi_{300\ K}+6.4\times10^{-5}$ (emu/mol). When $x'=0.5$, $n_h=0.5-x'=0$, thus χ_{Pauli} value is zero. So, the susceptibility of the three systems tends to converge at $\chi_{Pauli}=0$ when $x'=0.5$. However, the hole-filling dependence is quite different for the three systems. The susceptibility of the Zn-doped system decreases mildly at $x'<0.35$, but drops rapidly at the high doping level. The Cd-doped system exhibits the opposite case, and the In-doped system shows the steady decrease in the susceptibility.

The systematic variations on the hole-filling dependence of magnetic susceptibility suggests the band structure modi-

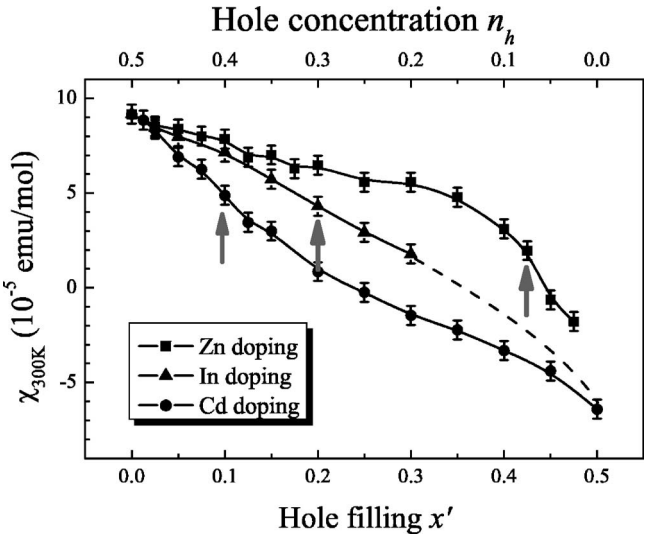

FIG. 6. Room-temperature susceptibility as a function of hole filling x' in the $Cu_{1-x}M_xIr_2S_4$ (M=Zn, In, and Cd) systems. The arrows mark the metal-semiconductor boundaries judged by the sign change of TCR at high temperatures. Note that $x'=x/2$ for the Zn-doped and Cd-doped systems.

fications upon the different doping, since $\chi_{\text{Pauli}}=\mu_B^2 N(E_F)$. First, there is a band narrowing effect mainly due to the distortion of the IrS_6 octahedra associated with the increase of the lattice constant. The Cd-doped system is expected to have the narrowest highest-occupying band. Second, the A-site doping induces Anderson-type disorder, which results in the distorted band tails. The Cd doping is expected to induce the strongest disorder potential, leading to the broadest band tail. Finally, the electron-phonon interactions enhanced by the band narrowing probably play an important role in the electronic localizations.

Although Anderson localization effect is responsible for the formation of the band tails, we argue that the Anderson-type localization is not the main mechanism for the semiconducting behavior at high temperatures for the relatively low hole-filling level (i.e., the Fermi level E_F is argued to be below the Mott mobility edges E_c at the low hole filling. However, at high hole-filling levels with relatively low hole concentrations, E_F level may go beyond the E_c edge, leading to the Anderson-type localization.[26]) This is because that the high-temperature $\rho(T)$ behavior of $Cu_{0.75}In_{0.25}Ir_2S_4$, for example, does not satisfy the expression of variable-range-hopping[15] of localized carriers, $\rho \propto \exp[(T_0/T)^{1/4}]$. The $\rho(T)$ curve in Fig. 4 actually suggests that small polaron formation is mainly responsible for the high-temperature semiconducting behavior.

One may be surprised at the fact that the high temperature $\chi(T)$ still exhibits Pauli paramagnetism for the $x=0.25$ sample (see Fig. 5). This can be explained as follows. For a localized electronic state in the nondegenerate limit, the $\chi(T)$ data should obey Curie's law. However, in the degenerate limit, as in the case of small-polaron narrow band, Pauli paramagnetism is still expected. Therefore, the $\chi_{300\ \text{K}}$ data does not show obvious changes in the metal-semiconductor boundaries shown in Fig. 6.

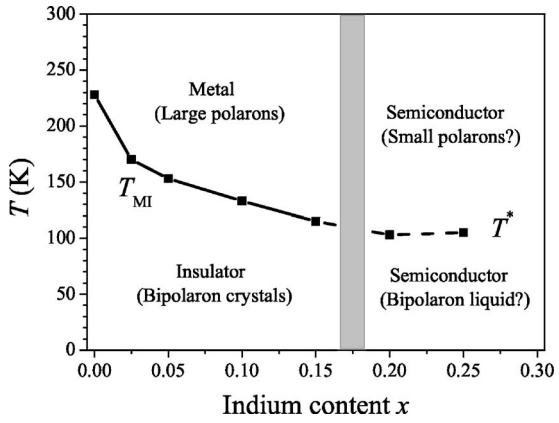

FIG. 7. Tentative electronic phase diagram in the $Cu_{1-x}In_xIr_2S_4$ spinel system. The solid line represents the first order transition, while the dashed line denotes the second order one. It is noted that the polaronic picture needs further confirmations.

D. Electronic phase diagram

The above results can be concluded in a tentative electronic phase diagram, as shown in Fig. 7. At the low doping level with $x \leqslant 0.2$, the high-temperature phase is metallic, which can be regarded as a large-polaron state if considered electron-phonon interactions. The low-temperature phase is in a charge-ordered and spin-dimerized insulating state, which can be described as bipolaron crystals. According to our results the transition from the large polarons to bipolaron crystals, which provides a possible explanation for the MI transition, would be of first order.

When the indium doping exceeds 0.2, the system shows the semiconductinglike behavior in the whole temperature range. The high-temperature semiconducting state can be elucidated in terms of small polarons, while the low-temperature semiconducting state is regarded as a bipolaron liquid. Based on our results the transition from the small polarons to small bipolarons, which explains the evolution of the MI transition, would be second order.

Since our results were obtained in polycrystalline samples, further experiments are needed to confirm the above polaronic features. In addition, it should be stated here that the bipolaron formation is only one possible scenario. Another possible explanation may come from the nanoscale phase separation that can be often seen in colossal magnetoresistence manganite system.[30] If one considers the coexistence of cubic and triclinic nanophases, both the drop of magnetic susceptibility at the T^* and the absence of thermal hysteresis in the $\rho(T)$ and $\chi(T)$ curves can also be explained.

E. Hole-depletion and lattice-size effects

Figure 8 plots the lattice constants and the phase transition temperatures in the $Cu_{1-x}M_xIr_2S_4$ (M=Zn, In, and Cd) system. Although all the doping on the Cu site depletes the holes in the metallic phase, the variations of T_{MI} or T^* are different. At the low hole-filling level up to $x'=0.025$, T_{MI} drops to about 175 K in all three systems. This implies that the suppression of the MI transition is mainly controlled by the hole depletion at the low doping level. The hole depletion

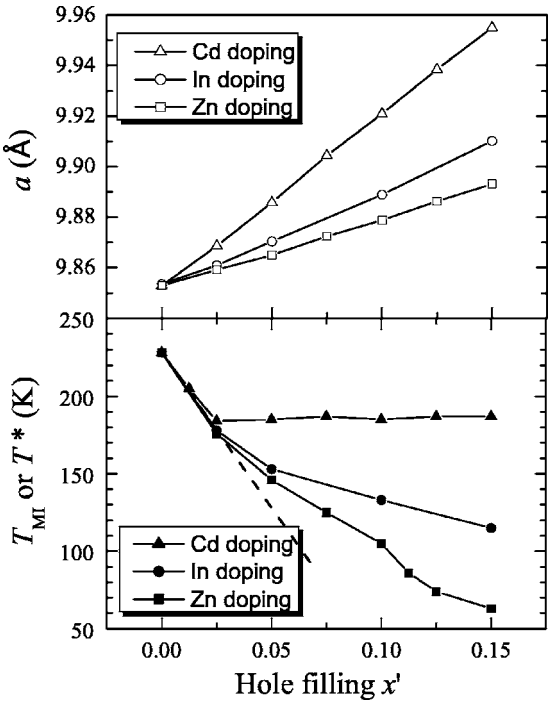

FIG. 8. Lattice-size and hole-filling effects on the MI transitions in the $Cu_{1-x}M_xIr_2S_4$ (M=Zn, In or Cd) system. The dashed line in the lower panel shows the tendency of T_{MI} for "pure" hole depletion.

for the parent compound means that the ratio of Ir^{4+} to Ir^{3+} deviates from 1:1, which is not in favor of the formation of the complex charge ordering (ordered bipolarons). In other words, the chemical doping induces extra electrons in the antibonding $d\varepsilon$ band for the dimerized Ir. As a result, T_{MI} is decreased rapidly by the hole depletion, depending hardly on the size of the dopants at the low doping level.

With the further hole depletion, the charge ordering cannot be maintained anymore, thus the disordered bipolaron state (for M=Cd or In) or the phase separation [for M=Zn (Ref. 13)] appears. When $x' > 0.025$, T_{MI} or T^* shows different hole-filling dependence. At a fixed hole-filling level, the larger lattice constant, the higher transition temperature. As discussed in Secs. III A and III C, larger lattice constant corresponds to narrower bandwidth for the valence bands. The energy band narrowing results in the enhancement of electron-phonon interactions, which stabilizes the polarons and the bipolarons.[31] Therefore, the lattice size effect on T_{MI} or T^* indicates that the electron-phonon coupling plays an important role in the MI transition in the present system.

It is also noted that superconductivity ground state was observed in the Zn-doped system for $x' \geqslant 0.125$. In the case of Cd and In doping, however, bipolaron liquid state appears at low temperatures for $x' \gtrsim 0.125$. According to the theoretical works,[32,33] Very strong electron-phonon interactions may lead to the transition from BCS Cooper pairs into small bipolarons. Therefore, the variations of the ground state due to the lattice size effect further suggest the existence of strong electron-phonon interactions in the thiospinel system.

IV. CONCLUSION

In conclusion, we have studied the thiospinel $Cu_{1-x}In_xIr_2S_4 (0 \leqslant x \leqslant 0.25)$ system by the measurements of crystal structure, electrical resistivity, and magnetic susceptibility. The structural analysis shows that indium preferentially occupies the Cu site. The In doping leads to the deviation of S—Ir—S bond angle from 90°, which weakens the $d\varepsilon$-p_π hybridization and makes the top valence band narrowed. It was shown that the In doping depletes the holes in the valence band of the high-temperature metallic phase, and induces extra electrons in the antibonding $d\varepsilon$ band for the insulating phase, suppressing the MI transition in the parent compound. By further doping up to $x \geqslant 0.2$, the MI transition evolves into a second-order semiconductor-to-semiconductor transition. The high-temperature semiconducting phase has the characteristic of small-polaron transport, while the low-temperature semiconducting phase has lower intrinsic magnetic susceptibility. Thus the semiconductor-to-semiconductor transition is argued to be associated with an electronic transformation from small polarons to small bipolarons. We also conclude that the systematic suppressions of the MI transitions in the $Cu_{1-x}M_xIr_2S_4$ (M=Zn, In or Cd) system are not only related to the hole depletions, but also linked with the strong electron-lattice coupling that is modulated by the band narrowing due to the large ionic size of the dopants. This observation implies that the MI transition in the parent compound is primarily due to a kind of lattice instability driven by the strong electron-phonon interactions.

ACKNOWLEDGMENT

This work was supported by the National Science Foundation of China (Grant No. 10104012).

*Author to whom correspondence should be addressed. Electronic address: ghcao@zju.edu.cn

[1] S. Nagata, T. Hagino, Y. Seki, and T. Bitoh, Physica B **194–196**, 1077 (1994).

[2] T. Furubayashi, T. Matsumoto, T. Hagino, and S. Nagata, J. Phys. Soc. Jpn. **63**, 3333 (1994).

[3] P. G. Radaelli, Y. Horibe, M. J. Gutmann, H. Ishibashi, C. H. Chen, R. M. Ibberson, Y. Koyama, Y. S. Hor, V. Kiryukhin, and S. W. Cheong, Nature (London) **416**, 155 (2002).

[4] G. Oomi, T. Kagayama, I. Yoshida, T. Hagina, and S. Nagata, J. Magn. Magn. Mater. **140–144**, 157 (1995).

[5] H. Kang, K. Bärner, I. V. Medvedeva, P. Mandal, A. Poddar, and E. Gmelin, J. Alloys Compd. **267**, 1 (1998).

[6] A. T. Burkov, T. Nakama, M. Hedo, K. Shintani, K. Yagasaki, N. Matsumoto, and S. Nagata, Phys. Rev. B **61**, 10049 (2000).

[7] J. Matsuno, T. Mizokawa, A. Fujimori, D. A. Zatsepin, V. R. Galakhov, E. Z. Kurmaev, Y. Kato, and S. Nagata, Phys. Rev. B **55**, R15979 (1997).

[8] M. Croft, W. Caliebe, H. Woo, T. A. Tyson, D. Sills, Y. S. Hor, S.-W. Cheong, V. Kiryukhin, and S.-J. Oh, Phys. Rev. B **67**, 201102(R) (2003).
[9] N. L. Wang, G. H. Cao, P. Zheng, G. Li, Z. Fang, T. Xiang, H. Kitazawa, and T. Matsumoto, Phys. Rev. B **69**, 153104 (2004).
[10] H. Ishibashi, T. Y. Koo, Y. S. Hor, A. Borissov, P. G. Radaelli, Y. Horibe, S.-W. Cheong, and V. Kiryukhin, Phys. Rev. B **66**, 144424 (2002).
[11] T. Furubayashi, H. Suzuki, T. Matsumoto, and S. Nagata, Solid State Commun. **126**, 617 (2003).
[12] H. Suzuki, T. Furubayashi, G. Cao, H. Kitazawa, A. Kamimura, K. Hirata, and T. Matsumoto, J. Phys. Soc. Jpn. **68**, 2495 (1999).
[13] G. Cao, T. Furubayashi, H. Suzuki, H. Kitazawa, T. Matsumoto, and Y. Uwatoko, Phys. Rev. B **64**, 214514 (2001).
[14] G. Cao, T. Naka, H. Kitazawa, M. Isobe, and T. Matsumoto, Phys. Lett. A **307**, 166 (2003).
[15] N. F. Mott, *Metal-Insulator Transitions* (Taylor and Francis, London, 1990).
[16] M. Imada, A. Fujimori, and Y. Tokura, Rev. Mod. Phys. **70**, 1039 (1998).
[17] K. Kitamoto, Y. Taguchi, K. Mimura, K. Ichikawa, O. Aita, and H. Ishibashi, Phys. Rev. B **68**, 195124 (2003).
[18] T. Oda, M. Shirai, N. Suzuki, and K. Motizuki, J. Phys.: Condens. Matter **7**, 4433 (1995).
[19] K. Kumagai, S. Tsuji, T. Hagino, and S. Nagata, in *Spectroscopy of Mott Insulators and Correlated Metals*, edited by A. Fujimori and Y. Tokura (Springer-Verlag, Berlin, 1995), p. 255.
[20] G. Y. Chitov and C. Gros, Phys. Rev. B **69**, 104423 (2004).
[21] T. Sasaki, M. Arai, T. Furubayashi, and T. Matsumoto, J. Phys. Soc. Jpn. **73**, 1875 (2004).
[22] S. Nagata, N. Matsumoto, Y. Kato, T. Furubayashi, T. Matsumoto, J. P. Sanchez, and P. Vulliet, Phys. Rev. B **58**, 6844 (1998).
[23] N. Matsumoto, R. Endoh, S. Nagata, T. Furubayashi, and T. Matsumoto, Phys. Rev. B **60**, 5258 (1999).
[24] R. Endoh, N. Matsumoto, S. Chikazawa, S. Nagata, T. Furubayashi, and T. Matsumoto, Phys. Rev. B **64**, 075106 (2001).
[25] R. Endoh, J. Awaka, and S. Nagata, Phys. Rev. B **68**, 115106 (2003).
[26] G. Cao, H. Kitazawa, T. Matsumoto, and C. Feng, Phys. Rev. B **69**, 045106 (2004).
[27] F. Izumi and T. Ikeda, Mater. Sci. Forum **321–324**, 198 (2000).
[28] D. Emin and T. Holstein, Ann. Phys. (N.Y.) **53**, 439 (1969).
[29] D. Emin, Phys. Rev. B **53**, 1260 (1996).
[30] E. Dagotto, *Nanoscale Phase Separation and Colossal Magnetoresistence* (Springer-Verlag, Berlin, Heidelberg, 2003).
[31] G. Iadonisi, C. A. Perroni, V. Cataudella, and G. De Filippis, J. Phys.: Condens. Matter **13**, 1499 (2001).
[32] B. K. Chakraverty, J. Phys. (Paris) **42**, 1351 (1981).
[33] K. Nasu, Phys. Rev. B **42**, 6076 (1990).